ELSEVIER

Fluid Dynamics Research 30 (2002) 155–168

FLUID DYNAMICS RESEARCH

The linear instability of a thermal boundary layer with suction in an anisotropic porous medium

D.A.S. Rees[a,*], L. Storesletten[a,b]

[a] *Department of Mechanical Engineering, University of Bath, Claverton Down, Bath, BA2 7AY, UK*
[b] *Department of Mathematics, Agder University College, Serviceboks 422, 4604 Kristiansand, Norway*

Accepted 5 December 2001

Abstract

We consider the combined effects of suction and transverse anisotropy on the instability of the uniform thickness boundary layer which is formed on an inclined heated surface in a porous medium. When the medium is isotropic, the stability characteristics are shown to be very similar to that of the inclined Darcy–Bénard problem. In particular, longitudinal rolls are always preferred, and transverse rolls are always stable when the inclination of the surface is greater than approximately 31.9°. Transverse anisotropy has no effect on the identity of the preferred mode of convection whenever the anisotropy parameter, ξ, is less than unity. When $\xi > 1$, there always exists a range of surface inclinations where transverse rolls are preferred. A detailed set of numerical results are given showing how the critical Rayleigh number and wavenumber vary with both inclination and ξ.

1. Introduction

The first studies concerned with the instability of free convective boundary layer flows in porous media appeared in the late 1970s. The pioneering works were carried out by Hsu et al. (1978) and by Hsu and Cheng (1979). Respectively, these authors considered the linear instability of horizontal and inclined boundary layers with respect to vortex disturbances. In both cases, neutral stability curves were obtained relating the critical distance, X_c, and the wavenumber of the vortices, where X_c is the distance from the leading edge beyond which disturbances grow. More detailed studies have appeared since, and the main reason is due to the variety of models which are frequently taken to

* Corresponding author. Tel.: +44-1225-826-775; fax: +44-1225-826-928.
E-mail address: ensdasr@bath.ac.uk (D.A.S. Rees).

0169-5983/02/$22.00
PII: S0169-5983(02)00035-7

Nomenclature

g	gravity
k	wavenumber
K_L	longitudinal permeability
K_T	transverse permeability
p	pressure
R	Darcy–Rayleigh number
t	time
T	temperature
u	fluid seepage velocity in the x-direction
v	fluid seepage velocity in the y-direction
V_w	surface suction velocity
w	fluid seepage velocity in the z-direction
x	Cartesian coordinate up the inclined layer
y	Cartesian coordinate normal to the layer
z	horizontal Cartesian coordinate across the layer

Greek symbols

α	layer inclination
β	coefficient of cubical expansion
κ	thermal diffusivity
μ	viscosity
ρ	reference density
σ	heat capacity ratio
ξ	anisotropy parameter
ϕ	orientation of roll
θ	scaled temperature
λ	complex exponential growth rate

Superscripts and subscripts

w	pertaining to the wall/surface
∞	pertaining to the ambient conditions
$*$	dimensionless
$'$	differentiation with respect to y
-	reduced disturbance quantities
0	basic flow
1	perturbation

describe convective flows in porous media. So far, then, there are about 30 publications devoted to instabilities and a comprehensive review of the subject has been presented by Rees (1998).

In this type of stability analysis, the first step is to determine a suitable representation of the basic flow using the boundary layer approximation. Then the governing equations are linearised about that basic flow. For disturbances of the form of longitudinal vortices, a spectral decomposition in the

spanwise direction is taken, while, for two-dimensional (transverse) waves a similar decomposition is used in the streamwise direction. The parallel flow approximation is assumed implicitly at this point, by which is meant in practice that the streamwise variation of the disturbance is specified, and the result of the linearisation is an ordinary differential eigenvalue problem for the critical distance as a function of the wavenumber of the disturbances.

In a recent paper, Storesletten and Rees (1998) re-examined the problems first considered in Hsu et al. (1978) and Hsu and Cheng (1979) for both horizontal and inclined surfaces. The novelty of their approach was that they tried to find a more accurate stability criterion by using asymptotic methods to obtain a better approximation to the basic steady boundary layer flow. However, they found that (i) the stability criterion is affected strongly by the external flowfield which is induced by the main boundary layer, and (ii) that instability occurs too close to the leading edge for the flow to be adequately represented by the higher order boundary layer theory described in their work. Thus, the main conclusion of Storesletten and Rees (1998) is that the use of traditional methods is usually quantitatively misleading. The one exception to this discouraging result is when the heated surface is close to the vertical: in this case the critical distance is very large and the boundary layer approximation is particularly accurate. Indeed, in this near-vertical limit, the full disturbance equations may be shown to satisfy the boundary layer approximation, and it is also possible to relax the parallel flow approximation and allow the disturbance to evolve in the streamwise direction. Some very recent linear vortex studies are given in Rees (2001) and nonlinear vortex studies in Rees (2002).

In the present paper, we consider the instability of flow induced by heated inclined surfaces but also consider the effects of (i) a lateral mass flux (suction) and (ii) anisotropy. The effect of suction on the basic boundary layer flow was studied in detail by Merkin (1978). The basic flow, if the surface has a well-defined leading edge, is nonsimilar but after a finite distance it becomes of uniform thickness and independent of the streamwise direction. Therefore, this type of boundary layer is not subject to the nonparallel-flow difficulties outlined in Rees (1998) as it bears a much greater mathematical relationship to the inclined Darcy–Bénard problem. This fact was one of the motivations for the present work since results obtained here will be precise for any inclination. The additional effect of anisotropy in the inclined Darcy–Bénard problem has been studied recently by Storesletten and Tveitereid (1999), Postelnicu and Rees (2001) and Rees and Postelnicu (2001). In Storesletten and Tveitereid (1999), the porous medium was assumed to be transversely isotropic (i.e. the permeabilities in the x- and z-directions are identical) and the authors found that transverse rolls were sometimes favoured over longitudinal rolls, unlike the case of an isotropic layer where longitudinal rolls are always favoured. In addition, they found that whenever transverse rolls are favoured, there is always a sudden transition to longitudinal rolls as the inclination of the layer increases. This is in contrast to the work contained in Rees and Postelnicu (2001) which considers more general anisotropies for which there may be a smooth transition in the preferred roll orientation as the inclination increases.

2. Mathematical formulation

We consider the instability of free convective boundary layer flow in a fluid-saturated anisotropic porous medium. The flow is induced by an isothermal, upward-facing and permeable surface which

is at an angle, α, to the horizontal, where $0^\circ \leqslant \alpha \leqslant 90^\circ$. The surface is held at a constant temperature, T_w, while the ambient temperature of the porous medium is T_∞ which satisfies $T_\infty < T_w$. Additionally, there is a normal fluid flux through the surface with velocity $-V_w$ where $V_w > 0$.

Cartesian coordinates (x, y, z) are orientated such that the y-axis is normal to the bounding surface, x is aligned up the surface, and z is the spanwise coordinate which also lies in the surface but is horizontal. Moreover, the porous medium is taken to be transversely isotropic in the permeability but homogeneously isotropic in its thermal diffusivity. The values K_L and K_T denote the longitudinal and transverse components of the permeability, where the x-direction is denoted as longitudinal. Darcy's law and the Oberbeck–Boussinesq approximation are assumed to be valid. The governing equations for unsteady three-dimensional flow are then,

$$\frac{\partial u}{\partial x} + \frac{\partial v}{\partial y} + \frac{\partial w}{\partial z} = 0, \tag{1a}$$

$$u = \frac{K_L}{\mu}\left[-\frac{\partial p}{\partial x} + \rho_\infty g\beta(T - T_\infty)\sin\alpha\right], \tag{1b}$$

$$v = \frac{K_T}{\mu}\left[-\frac{\partial p}{\partial y} + \rho_\infty g\beta(T - T_\infty)\cos\alpha\right], \tag{1c}$$

$$w = -\frac{K_T}{\mu}\frac{\partial p}{\partial z}, \tag{1d}$$

$$\sigma\frac{\partial T}{\partial t} + u\frac{\partial T}{\partial x} + v\frac{\partial T}{\partial y} + w\frac{\partial T}{\partial z} = \kappa\left[\frac{\partial^2 T}{\partial x^2} + \frac{\partial^2 T}{\partial y^2} + \frac{\partial^2 T}{\partial z^2}\right], \tag{1e}$$

where u, v and w denote the seepage velocities in the x-, y- and z-direction, respectively, p the pressure, T the temperature and t the time. Further, ρ_∞ denotes the density of the saturating fluid at $T = T_\infty$, μ its viscosity, and β the coefficient of cubical expansion. Lastly, g denotes gravity and σ is the ratio of the heat capacity of the saturated porous medium to that of the saturating fluid. The boundary conditions are

$$y = 0: \quad T = T_w, \quad v = -V_m, \tag{2a}$$

$$y \to \infty: \quad T \to T_\infty, \quad u \to 0. \tag{2b}$$

Merkin (1978) presented a boundary layer analysis of the basic flow and showed that it eventually attains a constant thickness due to the suction. Thus, the two-dimensional flow becomes independent of both x and z, and it takes the form,

$$u_0 = \frac{K_L}{\mu}\rho_\infty g\beta(T_w - T_\infty)\exp(-V_w y/\kappa)\sin\alpha, \tag{3a}$$

$$v_0 = -V_w, \quad w_0 = 0, \tag{3b}$$

$$T_0 = T_\infty + (T_w - T_\infty)\exp(-V_w y/\kappa). \tag{3c}$$

The governing equations are made dimensionless by setting

$$(u, v, w) = V_{\mathrm{w}}(u^*, v^*, w^*), \quad (x, y, z) = \frac{\kappa}{V_{\mathrm{w}}}(x^*, y^*, z^*), \tag{4a}$$

$$p = \frac{\kappa\mu}{K_{\mathrm{T}}}\, p^*, \quad T = T_\infty + (T_{\mathrm{w}} - T_\infty)\theta, \quad t = \frac{\sigma\kappa}{V_{\mathrm{w}}^2}\, t^*. \tag{4b}$$

The undisturbed basic flow now becomes,

$$u_0 = \xi(R\sin\alpha)\mathrm{e}^{-y}, \quad v_0 = -1, \quad w_0 = 0, \tag{5a}$$

$$\theta_0 = \mathrm{e}^{-y}, \quad p_0 = y - (R\cos\alpha)\mathrm{e}^{-y}, \tag{5b}$$

where R is the Darcy–Rayleigh number and ξ the anisotropy parameter which are given by

$$R = \frac{\rho_\infty g\beta K_{\mathrm{T}}(T_{\mathrm{w}} - T_\infty)}{\mu V_{\mathrm{w}}}, \quad \xi = \frac{K_{\mathrm{L}}}{K_{\mathrm{T}}}, \tag{6}$$

and where the asterisks introduced in Eq. (4) have been omitted in Eq. (5) and hereinafter for clarity of presentation. We note that Eq. (6) is not the usual definition of the Darcy–Rayleigh number for porous medium convection, but it may be made so if κ/V_{w} is adopted as the reference lengthscale.

By eliminating the velocity components from Eqs. (1), we eventually obtain the following dimensionless governing equations:

$$\xi\frac{\partial^2 p}{\partial x^2} + \frac{\partial^2 p}{\partial y^2} + \frac{\partial^2 p}{\partial z^2} = R\left[\xi\frac{\partial\theta}{\partial x}\sin\alpha + \frac{\partial\theta}{\partial y}\cos\alpha\right], \tag{7a}$$

$$\frac{\partial\theta}{\partial t} + R\left[\xi\frac{\partial\theta}{\partial x}\sin\alpha + \frac{\partial\theta}{\partial y}\cos\alpha\right]\theta - \xi\frac{\partial p}{\partial x}\frac{\partial\theta}{\partial x} - \frac{\partial p}{\partial y}\frac{\partial\theta}{\partial y} - \frac{\partial p}{\partial z}\frac{\partial\theta}{\partial z} = \frac{\partial^2\theta}{\partial x^2} + \frac{\partial^2\theta}{\partial y^2} + \frac{\partial^2\theta}{\partial z^2}, \tag{7b}$$

subject to the boundary conditions,

$$y = 0: \quad \theta = 1, \quad \frac{\partial p}{\partial y} = 1 + R\cos\alpha, \tag{8a}$$

$$y \to \infty: \quad \theta \to 0, \quad \frac{\partial p}{\partial y} \to 0. \tag{8b}$$

3. Stability analysis

The linear stability of the basic flow given by Eq. (5) may be investigated by setting

$$p = p_0(y) + p_1(x, y, z, t), \quad \theta = \theta_0(y) + \theta_1(x, y, z, t), \tag{9}$$

where the 1-subscript denotes infinitesimal disturbances. The substitution of Eq. (9) into the governing equations (7) followed by linearisation yields the following set of perturbation equations:

$$\xi\frac{\partial^2 p_1}{\partial x^2}+\frac{\partial^2 p_1}{\partial y^2}+\frac{\partial^2 p_1}{\partial z^2}=R\left[\xi\frac{\partial\theta_1}{\partial x}\sin\alpha+\frac{\partial\theta_1}{\partial y}\cos\alpha\right], \tag{10a}$$

$$\frac{\partial^2\theta_1}{\partial x^2}+\frac{\partial^2\theta_1}{\partial y^2}+\frac{\partial^2\theta_1}{\partial z^2}=R\mathrm{e}^{-y}\left[\xi\frac{\partial\theta_1}{\partial x}\sin\alpha-\theta_1\cos\alpha\right] -\frac{\partial\theta_1}{\partial y}+\mathrm{e}^{-y}\frac{\partial p_1}{\partial y}+\frac{\partial\theta_1}{\partial t}. \tag{10b}$$

We Fourier decompose the disturbances in the x- and z-directions which reduces the perturbation equations to ordinary differential eigenvalue form. We, therefore, substitute

$$p_1=\bar{p}(y)\exp[\mathrm{i}k(x\sin\phi+z\cos\phi)+\lambda t],$$
$$\theta_1=\bar{\theta}(y)\exp[\mathrm{i}k(x\sin\phi+z\cos\phi)+\lambda t], \tag{11}$$

into Eqs. (10a) and (10b) to obtain,

$$\bar{p}''-k^2(\xi\sin^2\phi+\cos^2\phi)\bar{p}=R[\mathrm{i}k\xi\sin\alpha\sin\phi\bar{\theta}+\cos\alpha\bar{\theta}'], \tag{12a}$$

$$\bar{\theta}''+\bar{\theta}'-k^2\bar{\theta}=R\mathrm{e}^{-y}[\mathrm{i}k\xi\sin\alpha\sin\phi\bar{\theta}-\cos\alpha\bar{\theta}]+\mathrm{e}^{-y}\bar{p}'+\lambda\bar{\theta}, \tag{12b}$$

where k is the wavenumber of the vortex, ϕ is the direction of its axis relative to the direction of the x-axis and λ is its growth rate. The boundary conditions are

$$y=0:\quad \bar{p}'=\bar{\theta}=0,\qquad y\to\infty:\quad \bar{p}',\bar{\theta}\to 0. \tag{13}$$

Eqs. (12a) and (12b) form an eigenvalue problem for R and $\mathrm{Im}(\lambda)$ as functions of ξ, α and k, given that $\mathrm{Re}(\lambda)=0$ corresponds to marginally stable disturbances. Therefore, it is necessary to supply normalisation conditions to enable computation of nonzero solutions of the homogeneous system (12) and (13):

$$\bar{\theta}'(0)=1. \tag{14}$$

As system (12) is complex, we have an eighth order system with two eigenvalues and 10 boundary conditions to satisfy in order to be able to compute the eigenvalues and eigenfunctions. A variety of numerical methods were used to solve these equations and these are described briefly in the following sections.

4. The isotropic case

Although much is known about the detailed behaviour of small disturbances to the inclined Darcy–Bénard layer, nothing is presently known about the corresponding suction layer. Therefore, it is essential to describe first the context into which the anisotropic results will be placed as these are presently unknown.

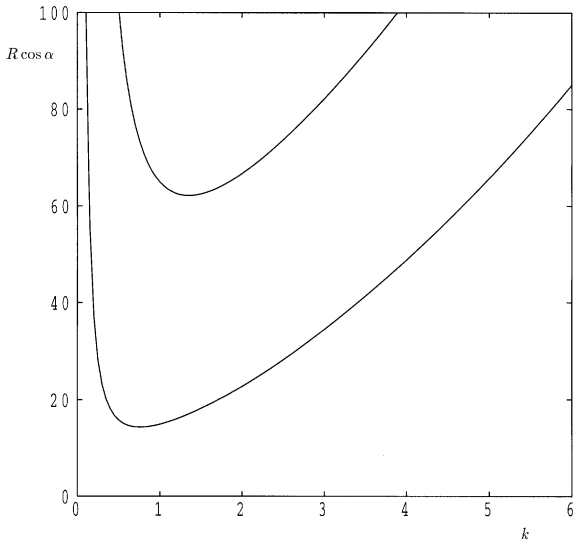

Fig. 1. The first two neutral curves for the onset of longitudinal modes in an isotropic porous medium.

In Fig. 1, we show the neutral curves corresponding to the first two modes of instability for longitudinal rolls where we display the variation of $R\cos\alpha$ with k. We note that these curves correspond to both the isotropic layer ($\xi = 1$) and to the more general anisotropic layers ($\xi \neq 1$), and, therefore, that R and α appear only in the combination $R\cos\alpha$. In this case Eqs. (12a) and (12b) are real when $\phi = 0$ and we solved the resulting boundary value problem using a straightforward fourth order Runge–Kutta scheme coupled to an algorithm which implements the shooting method. The curves display a well-defined minimum which, for the first mode is at $R\cos\alpha = 14.352$ and $k = 0.7589$, and, for the second mode, at $R\cos\alpha = 62.439$ and $k = 1.3478$; these values are correct to the quoted number of significant figures.

We note that it is possible to use the argument presented in the appendix of Rees and Bassom (2000) to prove that modes of other orientations arise at higher values of R for any given inclination. However, we also note that it is possible to suppress longitudinal modes by restricting the size of the physical domain in the z-direction using insulating impermeable sidewalls; in such cases it is possible for transverse rolls to become important. Moreover, given the fact that transverse rolls do assume importance when the layer is anisotropic, it is also very useful to know about their detailed behaviour for isotropic media. Therefore, Fig. 2 depicts the neutral curves for various inclination angles for the first three modes of instability. This figure was prepared using the matrix eigenvalue technique which is described in detail in Rees and Bassom (2000). The numerical method has the advantage that all neutral curves are guaranteed to be captured when the discretisation is sufficiently fine. In this case, we used 160 equally spaced intervals in the range $0 \leqslant y \leqslant 10$, and the figure showed no discernable difference from the one obtained using 80 intervals over the same range, or that using the same steplength over larger ranges. The neutral curves are displayed in terms of R (rather than $R\cos\alpha$) as a function of k. The first two modes (for $\alpha = 0$) are graphically identical to those displayed in Fig. 1, which cross-validates the two numerical methods.

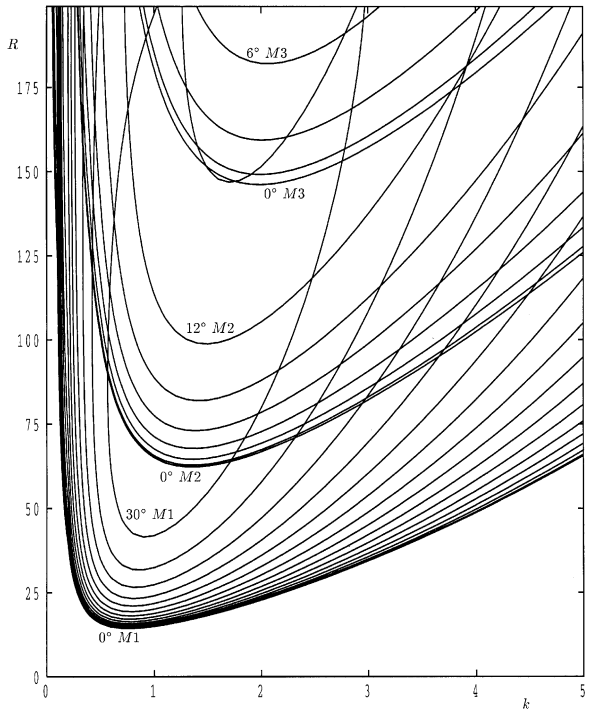

Fig. 2. Neutral curves for the onset of transverse modes in an isotropic porous medium for inclinations $\alpha=0^\circ, 2^\circ, 4^\circ, \ldots, 30^\circ$. Curves corresponding to the first three modes are shown. Modes 1, 2 and 3 are denoted by M1, M2 and M3, respectively.

It is clear that the critical value of R increases as the inclination increases, and eventually the closed curves disappear at an isola point at which $R \simeq 89.306^\circ$, $\alpha \simeq 31.861^\circ$ and $k \simeq 1.142$. These values may be compared with those for the inclined Darcy–Bénard channel: $R=104.296$, $\alpha=31.490^\circ$ and $k=2.555$ (taken from Rees and Bassom, 2000). The closeness of the critical Rayleigh numbers and of the inclination angles may be explained by appealing to the similarity between the respective flow configurations. But the great difference between the respective critical wavenumbers is caused by the fact that the nondimensional thicknesses of the respective layers are quite different. The thickness of the Darcy–Bénard layer is unity, while the thickness for the present problem could be taken to be the distance over which the basic temperature field (e^{-y}; see Eq. (5b)) reduces from 1 to 0.1, which is roughly 2.3. The variation of the critical Rayleigh number with inclination is shown in Fig. 3 and the corresponding wavenumber in Fig. 4. The maximum inclination for which neutral transverse modes exist is clearly visible and corresponds to the above value. At higher values of R, the curve corresponds to a maximisation over wavenumber which is depicted in Fig. 2 as the top of each closed loop. Above the closed loop transverse modes decay. Although we do not show the phenomenon here, the neutral transverse mode becomes thinner as R increases, and this means that the wavelength of the mode decreases (i.e. k increases) in order to maintain a cell aspect ratio which is roughly $O(1)$; this is shown quantitatively in Fig. 4.

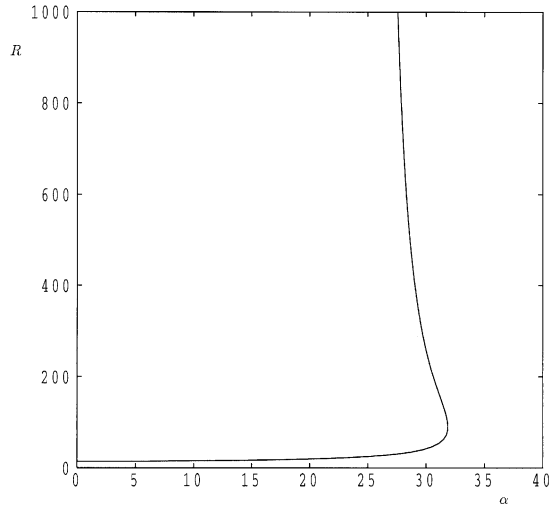

Fig. 3. The variation of the critical Rayleigh number with α for transverse modes in an isotropic medium. The points below the turning point correspond to minima in the first mode neutral curves displayed in Fig. 2, while the points above are maxima.

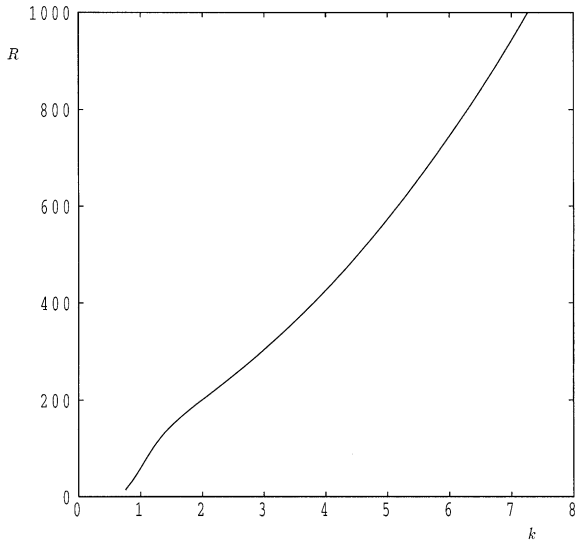

Fig. 4. The variation of the minimising wavenumber k with R for transverse modes in an isotropic medium. This curve corresponds to that shown in Fig. 3. We have chosen R to be the ordinate in order to facilitate direct comparison with Fig. 3.

5. The anisotropic case

When the porous medium is anisotropic, but transversely isotropic as in Storesletten and Tveitereid (1999), the Darcy–Bénard layer has the property that the most unstable mode is either the longitudinal

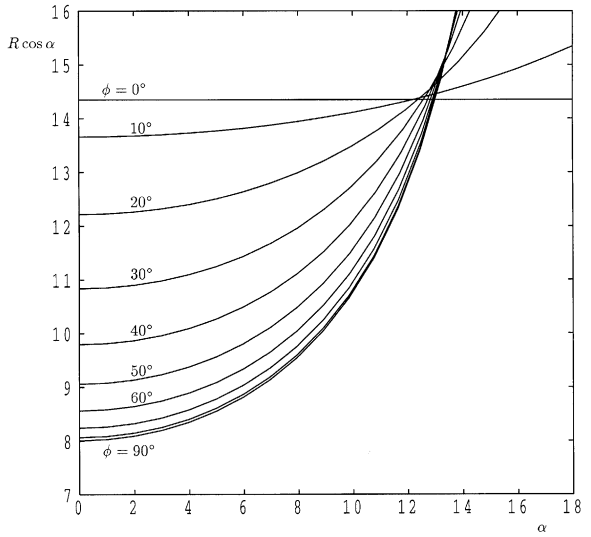

Fig. 5. The critical Rayleigh number as a function of inclination, α, when $\xi = 5$, for roll orientations, $\phi = 0^\circ, 10^\circ, \ldots, 90^\circ$. The angle $\phi = 0^\circ$ corresponds to longitudinal rolls, while $\phi = 90^\circ$ corresponds to transverse rolls.

roll ($\phi = 0^\circ$) or the transverse roll ($\phi = 90^\circ$). The identity of the preferred mode depends on the precise value of the anisotropy parameter, ξ, and the inclination angle, α. At the outset it is essential, therefore, to check carefully whether this property is shared by the present configuration.

This was undertaken by solving Eqs. (12a) and (12b) in exactly the same manner as were the corresponding equations in Rees and Postelnicu (2001). Thus, we differentiated Eq. (12a) to obtain a second-order equation for $\bar{p}'$ as this function satsifies Dirichlet boundary conditions and numerical solutions using such boundary conditions yield more accurate solutions for a given number of grid points. The discretisation used $y_{\max} = 10$ and 200 equally spaced intervals. The method is a variant of the Keller-box method and is adapted to solve eigenvalue problems based on discretisations of systems of second-order equations. In this case, we have solved the appropriate system of equations which yields the minimum (and maximum) values of the neutral curves. Again, the numerical solutions obtained compare extremely well with the numerical data corresponding to those displayed in Figs. 1 and 2, which provides further validation of the accuracy of the encoding of each method.

In Fig. 5, we display the neutral curves (minimised with respect to k) for rolls of various orientations between $\phi = 0^\circ$ and 90°. For the case $\xi = 5$, we have plotted $R\cos\alpha$ against α—the reason for this is because the longitudinal mode then corresponds to a horizontal line. In this figure, we see quite clearly that there is again an abrupt transition between transverse rolls at relatively small inclinations and longitudinal rolls at higher inclinations. A similar behaviour was found for all cases for which $\xi > 1$; whenever $\xi < 1$ longitudinal modes are always favoured. These stability characteristics are not surprising, given the results of Storesletten and Tveitereid (1999), but in the light of the computations presented in Rees and Postelnicu (2001) we think it likely that smooth transitions could occur for more general anisotropies.

Given the general behaviour illustrated by Fig. 5, it is necessary only to present curves corresponding to transverse modes for various values of ξ and to show how they compare with the

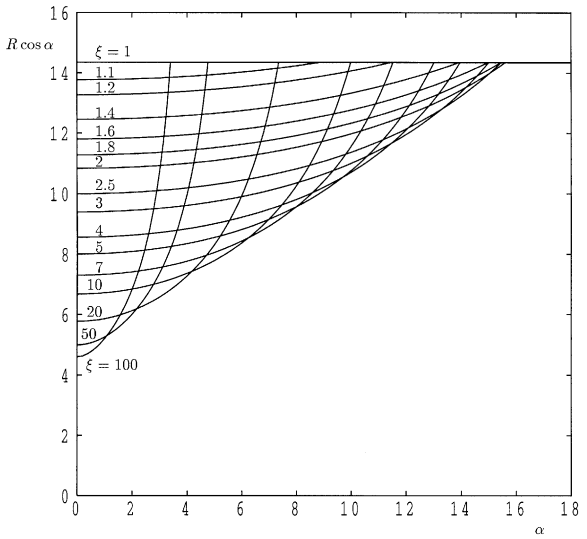

Fig. 6. The variation of the critical Rayleigh number corresponding to the most dangerous mode. The straight line corresponds to the longitudinal mode while more dangerous transverse modes for various values of ξ correspond to the other curves.

curve for the longitudinal mode which is independent of ξ. Such a general comparison is given in Fig. 6, where we show neutral transverse mode curves for various values of ξ which are again minimised with respect to the wavenumber. When ξ is just above 1 there is only a small range of inclinations near the horizontal in which transverse modes dominate. As ξ increases, this range of inclinations increases to a maximum ($0 \leqslant \alpha < 15.614^{\circ}$) at $\xi = 2.107$, after which it decreases again. For large values of ξ, flow in the x-direction is enhanced greatly because of the relatively large permeability, and therefore the critical value of R (when α is small) decreases as ξ increases. The corresponding critical wavenumbers are shown in Fig. 7, and these generally decrease with increasing values of ξ.

Finally, in Fig. 8, we show the variation with ξ of the inclination at which the transverse mode has the same critical Rayleigh number as the longitudinal mode. This curve is an important summary of the linear stability characteristics of the basic flow since points below the curve correspond to where transverse modes dominate, while points above and to the left correspond to cases where longitudinal modes form the dominant instability. The general shape of this curve is as described in the previous paragraph, and some transitional values of α for larger values of ξ are given in Table 1.

6. Conclusions

We have considered the onset of convection in a porous medium where the inclined bounding surface is held at a uniform temperature above the ambient and through which fluid is sucked at a uniform rate. The basic flow is uniform and is a function of y, the coordinate perpendicular to the surface. We have considered the relative importance of longitudinal and transverse modes of

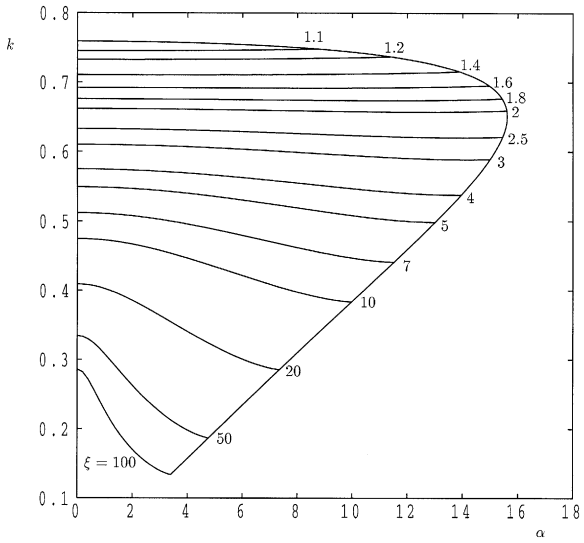

Fig. 7. The variation of the critical wavenumber corresponding to the most dangerous transverse mode. The curves shown correspond to the same values of ξ as in Fig. 6. Also shown is the envelope of critical wavenumbers corresponding to that inclination at which longitudinal and transverse modes have the same critical Rayleigh number. The critical wavenumber for longitudinal modes is 0.7589 which corresponds to the intercept of the envelope curve with the k-axis.

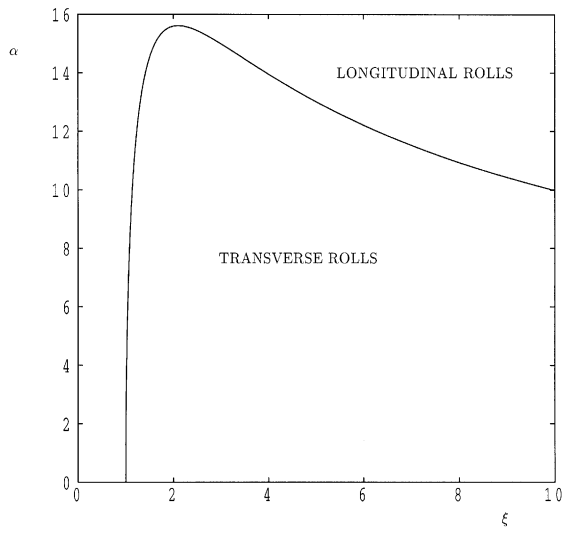

Fig. 8. Delineation of α–ξ-space into those regions for which transverse and longitudinal modes form the preferred mode at onset.

instability and, in particular, how the balance between these is affected by the presence of anisotropy. We have found that one or other of these modes always dominates, rather than having modes of other orientations, and that there is always an abrupt transition in the identity of the most dangerous

Table 1
Values of ξ and α at which the critical values of R for longitudinal and transverse modes are the same

ξ	α
1.001	0.972°
1.010	3.046°
1.100	8.830°
1.500	14.539°
2.107	15.614°
5.000	13.013°
10.000	9.981°
15.000	8.373°
20.000	7.350°
30.000	6.084°
40.000	5.305°
50.000	4.764°
60.000	4.361°
70.000	4.046°
80.000	3.790°
90.000	3.577°
100.000	3.397°

mode—see Fig. 5 which shows how the critical Rayleigh numbers of modes of various orientations vary with inclination. We note that the overall situation is summed up in Fig. 8 which delineates the separate regions in which the respective modes dominate, and in Table 1.

Acknowledgements

L.S. gratefully acknowledges financial support from the Norwegian Research Council during his sabbatical leave at the University of Bath, Autumn 2000.

References

Hsu, C.T., Cheng, P., 1979. Vortex instability in buoyancy induced flow over inclined heated surfaces in porous media. Trans. A.S.M.E. J. Heat Transfer 101, 660–665.

Hsu, C.T., Cheng, P., Homsy, G.M., 1978. Instability of free convection flow over a horizontal impermeable surface in a porous medium. Int. J. Heat Mass Transfer 21, 1221–1228.

Merkin, J.H., 1978. Free convection boundary layers in a saturated porous medium with lateral mass flux. Int. J. Heat Mass Transfer 21, 1499–1504.

Postelnicu, A., Rees, D.A.S., 2001. The onset of convection in an anisotropic porous layer inclined at a small angle from the horizontal. Int. Commun. Heat Mass Transfer 28 (5), 641–650.

Rees, D.A.S., 1998. Thermal boundary-layer instabilities in porous media: a critical review. In: Ingham, D.B., Pop, I. (Eds.), Transport Phenomena in Porous Media. Pergamon, New York, pp. 233–259.

Rees, D.A.S., 2001. Vortex instability from a near vertical heated surface in a porous medium. I. Linear instability. Proc. R. Soc. London 457, 1721–1734.

Rees, D.A.S., 2002. Vortex instability from a near vertical heated surface in a porous medium. II. Nonlinear evolution. Proc. R. Soc. London, to appear.

Rees, D.A.S., Bassom, A.P., 2000. Onset of Darcy–Bénard convection in an inclined porous layer heated from below. Acta Mech. 144, 103–118.

Rees, D.A.S., Postelnicu, A., 2001. The onset of convection in an inclined anisotropic porous layer. Int. J. Heat Mass Transfer 44, 4127–4138.

Storesletten, L., Rees, D.A.S., 1998. The influence of higher-order effects on the linear instability of thermal boundary layer flow in porous media. Int. J. Heat Mass Transfer 41, 1833–1843.

Storesletten, L., Tveitereid, M., 1999. Onset of convection in an inclined porous layer with anisotropic permeability. Appl. Mech. Eng. 4, 575–587.